euspen's 26th International Conference & Exhibition, Krakow, PL, June 2026
www.euspen.eu

On-machine optical tool characterisation using dictionary-based sub-pixel edge detection

Moritz Genzwürker[1], Matthias Geiselhart[1], Giuliano Bissacco[1]

[1] *Technical University of Denmark, Department of Mechanical Engineering, 2800 Kgs. Lyngby, Denmark*

morge@dtu.dk

Abstract

An on-machine optical measurement system is developed for 3D reconstruction of spindle-mounted rotating cutting tools, addressing the need for near real-time cutting-edge geometry data to support surface generation prediction in precision machining. The system is calibrated on the machine and achieves sub-pixel resolution in the direction perpendicular to the edge profile. A novel on-machine camera alignment process based on a spherical artefact facilitates the measurement process. Performance evaluation following ISO 15530-3 is carried out, yielding an expanded uncertainty of 9.8 µm (k=2) and a repeatability of 0.074 µm for radius measurements. The system is shown capable of reconstructing cutting-edge profiles and quantifying radius and runout. The primary error source is a systematic bias of 4.8 µm, which, if corrected, could significantly improve system performance.

Machining, Measuring instrument, Precision, Tool

1. Introduction

In precision manufacturing, the quality of machined surfaces directly determines component functionality, service life and production cost. With industries pushing towards tighter tolerances and higher requirements regarding surface integrity, the ability to predict and control surface topography has become a critical competitive factor.

High-fidelity surface generation prediction for finishing milling operations requires high-resolution information on the morphology of the cutting edges engaging the workpiece surface. High-resolution cutting-edge characterisation is possible using off-machine instruments such as optical profilometers [1]. However, the cutting-edge morphology changes during machining operations, and so does the topography of the generated surfaces [2-3]. Thus, in order to exploit surface generation models in production, it is vital to provide them with real-time information on the cutting edges' morphology in their current condition. Automated on-machine tool measurement systems exist in the form of laser beam interruption systems, laser scan micrometres and camera systems [4]; however, these are either incapable of characterising the full profile of the cutting edges or do not currently deliver sufficient resolution to facilitate high-fidelity wear monitoring and edge morphology characterisation.

This paper presents the initial steps in the development of an optical on-machine tool measurement system capable of reconstructing the 3D cutting-edge geometry of endmills of generic profile geometries. A novel variant of dictionary-based sub-pixel edge detection is introduced, where the reference profiles are generated from CNC-controlled motion of an uncalibrated artefact. Section 2 details the system design, including an on-machine camera alignment strategy, calibration and post-processing methodology. Section 3 presents a metrological evaluation of the prototype system in accordance with ISO 15530-3. Section 4 concludes the paper and outlines directions for future work.

2. System Design and Methodology

2.1 Setup

Figure 1 shows the experimental setup inside the working envelope of a FANUC ROBODRILL α-D21LiB5adv. A Basler a2A1920-160umBAS greyscale global shutter camera with a VS-TCH1.5-65 telecentric lens is mounted opposite a collimated light source (green LED) in a shadowgraph-like setup. The camera pulses the LED for 10 µs per exposure using an EU-38-TTL LED driver to reduce the effective shutter speed and observed motion blur. The setup is connected to a power supply and PC outside the machine.

Spindle-mounted cutting tools smaller than the camera's field of view of 4.5 x 2.8 mm are moved to their measurement position (determined as described in Section 2.2) using the machine's linear drives. The camera captures silhouette images of the cutting tool at a sampling frequency determined using Equation 1. This is to compensate for the spindle speed, ω, being many times faster than the camera's maximum sampling frequency, $\mathrm{fps_{max}}$, of 160 Hz. Images of the tool are captured over multiple rotations with a known angular step and appear in order of orientation. Here, ω is the spindle speed and k the number of revolutions between images to enable the desired angular resolution, α.

$$\mathrm{fps(k)} = \frac{\omega \cdot 2\pi}{\alpha + 2\pi \cdot k} < \mathrm{fps_{max}}, \quad k = 0,1,2,.. \tag{1}$$

Figure 2 shows images of two spindle-mounted artefacts captured at 6000 rpm using the setup (a flat endmill and a square bar). The chosen camera/lens combination gives the system an image scale of 2.3 µm px^{-1}. This is far too coarse for high-accuracy edge profile characterisation. Section 2.4, therefore, introduces a novel approach to on-machine camera calibration and sub-pixel interpolation.

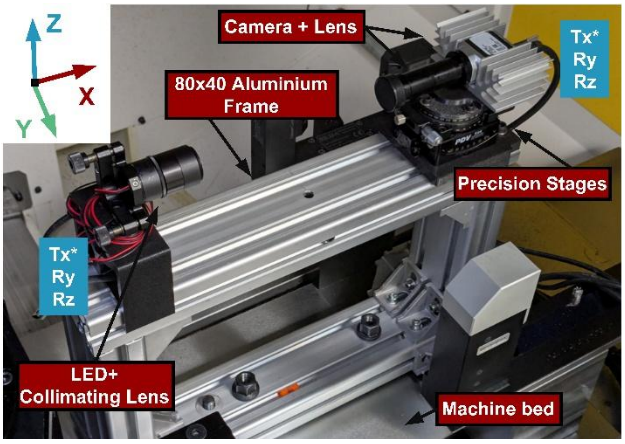

Figure 1. Experimental setup inside the CNC machine. The camera and backlight are mounted on precision manual stages, facilitating rotation around the Y and Z axes. Both components can be moved along the X-axis to tune the illumination distance.

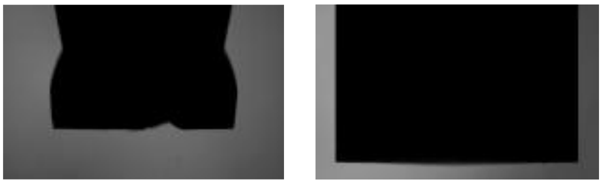

a) b)

Figure 2. Silhouette images captured by the system of a) a 3 mm, four-fluted flat endmill and b) a square bar at 6000 rpm.

2.2 Locating the focal plane

Extraction of accurate, repeatable data from the acquired images requires that the tool be in optimal focus. This occurs when the spindle axis lies on the lenses' focal plane. Here, due to the geometry of cutting tools, the outermost segments of the cutting edges appear maximally sharp (as seen in Figure 2a).

The focal point of the optical system is located within the machine tool working volume using a tube-mounted Ø 12 mm uncalibrated steel sphere fixed in a tool holder and clamped to the spindle. The exact geometry of the sphere is not critical since no dimensional information from it will be used to inform the measurement process. The layout is shown in Figure ***3***.

From the camera's perspective, the sphere appears as a circular silhouette regardless of alignment. The silhouette's perimeter is most in focus when the spindle axis intersects the focal plane. The focal point (ideal measurement position along the optical axis) can hence be determined using a Sobel Gradient-based focus measure, along the perimeter of the sphere projection, computed according to Equation 2.

$$\mathrm{F_{edge}} = \frac{1}{N} \sum_{(i,j) \in \mathrm{edge}} (G_i(i,j)^2 + G_j(i,j)^2) \quad (2)$$

Where (i, j) are pixel coordinates, I the local intensity and $G_i \approx \frac{\partial I}{\partial i}$ and $G_j \approx \frac{\partial I}{\partial j}$ are the derivatives of intensity in two orthogonal directions. The sphere is then swept along the X axis of the machine until a peak in $\mathrm{F_{edge}}$ is detected. The X position of the spindle is recorded and used to position the cutting tools during subsequent measurements. To compensate for runout, the sphere is rotated at low rpm during this process.

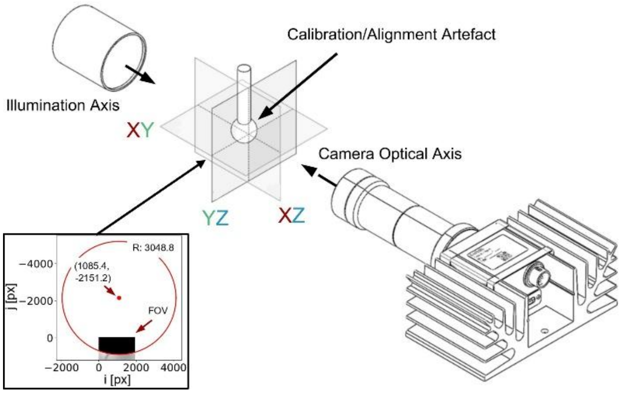

Figure 3. Setup for focusing, alignment and calibration of the optical system using a Ø 12 mm spindle-mounted sphere.

2.3 Focal plane alignment with machine axes

To facilitate on-machine calibration, the camera's focal plane must be aligned with the CNC machine's YZ plane. This is achieved via a live post-processing script that fits a circle to the visible parts of the sphere's silhouette (see Figure 3). The centre position of the sphere is then easily traceable at sub-pixel resolution. When the camera is correctly aligned (i.e. the X axis is parallel with the optical axis), sweeping the sphere along the machine's X axis should not change its centre position (beyond minor fluctuations due to vibrations). Drift of the tracked centre caused by motion of the sphere along the X axis can be corrected using the set precision stages (see Figure ***1***). This enables fine-tuning of the camera's alignment to within approximately 0.12 deg. The main limitation in this process is currently the backlash in the stages. This will be mitigated with a better mechanical alignment solution in the future.

2.4 Calibration and edge detection

During initial testing, a pixel-level attempt was made to reconstruct the 3D cutting-edge geometry of a cutting tool from images acquired by the system. A series of 400 silhouette images of the endmill shown in Figure 2a, rotating at 6000 rpm were captured using the system. One point per cutting edge per frame was extracted (in pixel coordinates), where the cutting edge was most in focus. This point was identified as the pixel with the maximum magnitude of the intensity gradient in the direction normal to the edge. Since the rotation of the tool between images is known (angular resolution, α), these points can be used to generate a point cloud representing the cutting tool. The result is shown in Figure 4.

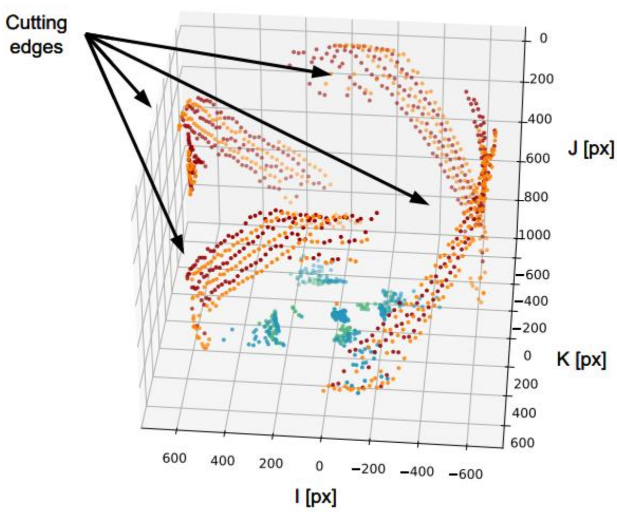

Figure 4. Preliminary 3D reconstruction of the flat endmill shown in Figure 2a at pixel-level.

However, to facilitate tool presetting and surface prediction, geometric data finer than the image scale is needed. This requires calibration of the camera and the implementation of an edge detection algorithm and a sub-pixel interpolation method. A multitude of techniques exist in this field, with different sensitivities and accuracies.

A common method is dictionary-based sub-pixel edge detection, where local image neighbourhoods are matched against preexisting edge profiles with known sub-pixel offsets. This method is often used in high-precision vision applications with computationally generated reference edge profiles. The main pitfall of this method is that the reference profiles are created based on assumptions regarding the optics and generally do not capture, e.g. non-uniformities in the illumination or lens imperfections.

To circumvent these limitations, the prototype system exploits the CNC machine's high-precision movements to generate a set of true reference profiles that represent the unique characteristics of the optical components.

With the camera aligned with the machine axes, the sphere is initially swept in the positive Y direction across the field of view at a constant feed (0.9 mm min^{-1}). The camera captures this motion at 150 Hz, creating a dataset of the sensor's response to right-facing edges (dark→light, left→right as seen by the camera) in 100 nm steps. This process is illustrated in Figure 5. Repeating the above by sweeping the sphere in the negative Y direction, as well as the negative Z direction, builds a full dictionary of the system's response to all edges around the perimeter of spindle-mounted objects. The proposed method encodes lens aberrations, illumination gradients, and scattering directly into the dictionary, eliminating model-dependent errors.

During post-processing of the tool data, the edge profiles are compared with the profile dictionary generated from the sphere's motion. The comparison is performed according to Equation 3 (cosine similarity). Where $V_{I.tool}$ is a 1D vector containing the intensity across the edge profile of the measured tool in a given pixel row or column, and $V_{I.reference}$ is the library of edge profiles for that row or column.

Figure 6 shows the edge profile over the left-facing edge of a cutting tool (black) overlaid with the most similar edge profile acquired during the passing of the sphere (blue). The index of the most similar profile, together with the known spacing of the reference profiles (100 nm), is then used to back-calculate the edge position. The conversion assumes constant feed during the generation of the reference profiles.

$$\text{Similarity} = \frac{V_{I.tool} \cdot V_{I.reference}}{\|V_{I.tool}\| \|V_{I.reference}\|} \quad (3)$$

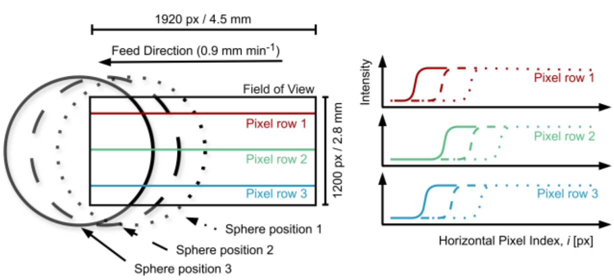

Figure 5. Illustration of the on-machine camera calibration process during creation of the right-facing edge dictionary. The horizontal intensity profiles, shown here for three arbitrary rows at three time steps, are extracted and used as reference profiles. (The size of the sphere is not to scale)

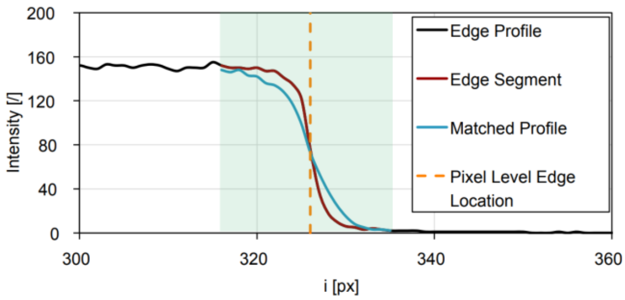

Figure 6. Intensity profile across the left edge of a cutting tool overlaid with the most similar profile (determined according to Equation 3) from the calibration process.

This method improves the system's edge localisation precision, yielding finer measurements in the radial direction of the tool and of tool length. However, on its own, the proposed approach cannot improve the measurement point density along the cutting edges, which remains constrained to the image scale of 2.3 µm px^{-1}. The development of a method to increase axial measurement resolution is left for future work.

2.5 Artefact measurement

Figure 7 shows the edge detection process applied to 400 images captured of a calibrated artefact with a square cross-section (Figure 2b) rotating at 6000 rpm. The left-facing edge profiles, 0.261 mm from the bottom surface in each image, were compared to the dictionary and converted to distances from the spindle axis in millimetres.

As Figure 7 shows, two full revolutions of the square bar were captured. The runout of the rotating artefact is clearly visible, as the difference between the longest and the shortest edge. The plot is overlaid with the cosine similarity (Equation 3), whose peaks coincide with those in the distance from the spindle axis. This should be the case because the edges will be most in focus (i.e., better agreement between the dictionary data and the instantaneous edge profile) when one of the diagonals of the square is aligned with the focal plane.

Applying this edge detection process to all pixel rows and columns, and assuming a constant spindle speed during the measurement, will enable the generation of a 3D point cloud visualising the edge geometry. The reconstruction will have a measurement resolution determined by the 100 nm dictionary spacing and an axial resolution constrained by the image scale, appearing similar to Figure 4.

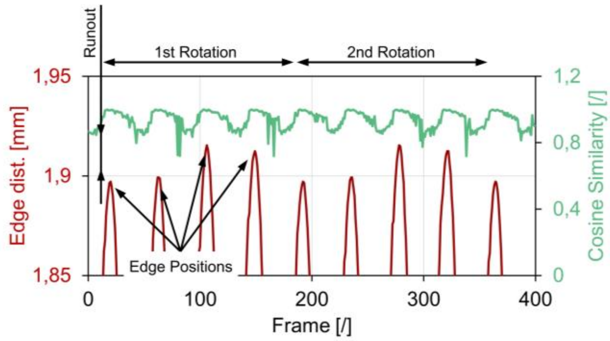

Figure 7. Post-processing of the left-facing edges from images of the square bar from Figure 2b.

3. System Evaluation

The metrological performance of the prototype system was assessed by characterising the edge position and runout of the square bar shown in Figure 2b at an axial position 0.261 mm from its bottom face. Reference values were obtained from prior artefact calibration [5], though it should be noted that the artefact was calibrated off-machine, meaning that clamping errors during mounting in the spindle will have affected the accuracy of the reference data.

All measurements were performed after a 30-minute thermal stabilisation period with the spindle running at the measurement speed (6000 rpm). In accordance with ISO 15530 part-3 [6], twenty repeated measurements were used to establish the system's repeatability. Between measurements, the spindle was moved to the top of its Z-axis range and returned to the measurement position.

Table 1 summarises the results. The largest edge radial distance was recorded at 1.9151 mm, with a repeatability of 0.074 µm. The runout, calculated as the difference between the largest and smallest edge radii, came to a mean of 24.081 µm, with a repeatability of 0.178 µm.

Figure 8 shows the average of the measured distances of the four edges from the spindle axis as measured by the system over the 20 trials, compared to the reference measurements from [5].

Following ISO 15530 part-3 [6] and the method proposed in [5], the expanded measurement uncertainty was evaluated as U_M = 9.8 µm (k=2, 95.45 % confidence interval). This value is obtained by calculating the uncertainty for each individual artefact edge and taking the largest one. As per the standard, the uncertainty accounts for the random and systematic errors summarised in Equation 4.

$$U_M = k\sqrt{u_{cal}^2 + u_b^2 + u_p^2 + u_w^2} \quad (4)$$

Here, u_{cal} is the standard uncertainty of the square artefact of 0.74 µm [5], u_b is the systematic error obtained as the difference between the average measurement and the reference value, $u_p = s/\sqrt{n}$ (where s is the standard deviation across repeated measurements and n the number of samples) and u_w the workpiece variation during use. Because the measurements were carried out in immediate succession, it is assumed that there is no variation. The contribution of u_p is calculated to 0.04 µm. Systematic bias contributes 4.8 µm to the uncertainty and could, if corrected, drastically improve the system's performance. The main contributors to the bias are likely residual camera misalignment and rotation blur mismatch, since the dictionary is built from a non-rotating object with minimal motion blur, but the artefact is measured at high rpm.

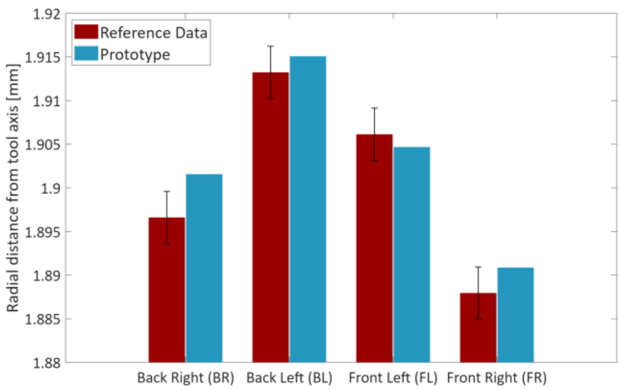

Figure 8. Cutting-edge radii measured by the prototype system (purple) compared to reference data from [5].

Table 1. Data from 20 repeated measurements of the square artefact, 0.261 mm from its bottom face.

Largest Radius		Runout	
Average	Repeatability	Average	Repeatability
1.9151 mm	0.074 µm	24.081 µm	0.178 µm

4. Conclusions and Future Work

This work demonstrates that generating an edge-response dictionary in situ from CNC-controlled motion of a geometrically undefined artefact offers a viable path towards high-resolution on-machine tool characterisation. The prototype system achieved an expanded measurement uncertainty of 9.8 µm for edge position measurements on a calibrated square bar, which could be reduced significantly upon correction of the 4.8 µm systematic bias. The system's repeatability is 0.074 µm over a set of twenty measurements.

The system would be suitable for industrial pre-setting applications, but will be expanded in the future to improve its performance in edge-profile characterisation for wear measurement in fine-finishing operations.

References

[1] F. G. Biondani and G. Bissacco, "Effect of cutting edge micro geometry on surface generation in ball end milling," *CIRP Annals*, vol. 68, no. 1, pp. 571–574, Jan. 2019, doi: 10.1016/j.cirp.2019.04.017.

[2] A. Shaheen, Ø. Svinning, I. Nedrehagen, and G. Bissacco, "On-machine high accuracy radial wear characterization of rotating milling tools using a camera-based system," *J Manuf Process*, vol. 157, pp. 62–77, Jan. 2026, doi: 10.1016/j.jmapro.2025.11.064.

[3] B. Denkena and D. Biermann, "Cutting edge geometries", doi: 10.1016/j.cirp.2014.05.009.

[4] W. Wang, W. Liu, Y. Zhang, Y. Liu, P. Zhang, and Z. Jia, "Precise measurement of geometric and physical quantities in cutting tools inspection and condition monitoring: A review," 2023, doi: 10.1016/j.cja.2023.08.011.

[5] A. Shaheen and G. Bissacco, "Metrological characterisation of tool pre-setting optical systems based on 2D imaging," *Measurement (Lond)*, vol. 228, Mar. 2024, doi: 10.1016/j.measurement.2024.114327.

[6] "ISO 15530-3:2011 - Geometrical product specifications (GPS) — Coordinate measuring machines (CMM): Technique for determining the uncertainty of measurement — Part 3: Use of calibrated workpieces or measurement standards." Accessed: Jan. 10, 2026. [Online]. Available: https://www.iso.org/standard/53627.html